Mammographically Configured, Automated Ultrasound: Methods and Potential Applications

Paul L. Carson, Ph.D.

Marilyn A. Roubidoux, M.D., Mitchel A. Goodsitt, Ph.D., Oliver Kripfgans, Ph.D., Won-Mean Lee, M.S., Rungroj Jintamethasawat, M.S., Brian Fowlkes, Ph.D., Chris Lashbrook, RT, Fong Ming Hooi, Ph.D., Xueding Wang, Ph.D., et al.

University of Michigan

Peng Gu, B.E., Jie Yuan, Ph.D.

Nanjing University

AAPM, July 15, 2015

The most promising imaging modality for improved breast screening - automated breast US

- False positives are a problem
- 3 geometries
- Supine for US plus optical imaging
  - Not collocated with dependent or compressed breast
- Conventional mammographic geometry
  - US with Breast Tomography & Optical/Photoacoustic
- Dependent breast in air or water
  - US with MRI/X-ray CT & Optical/Microwave

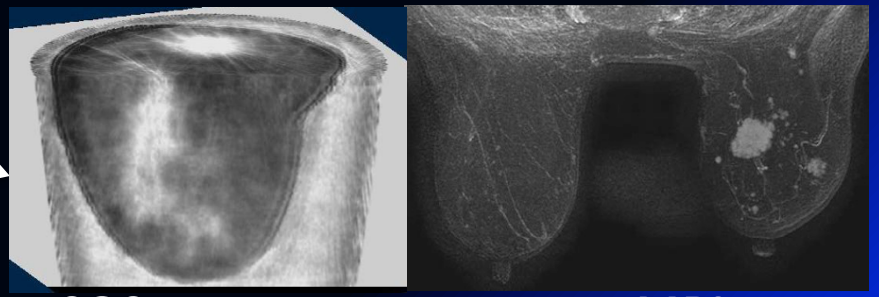

SOS **MRI**

Karmanos Ca Inst., N Duric

Breast Light and Ultrasound Combined Imaging (BLUCI)

Two of the 3 systems discussed

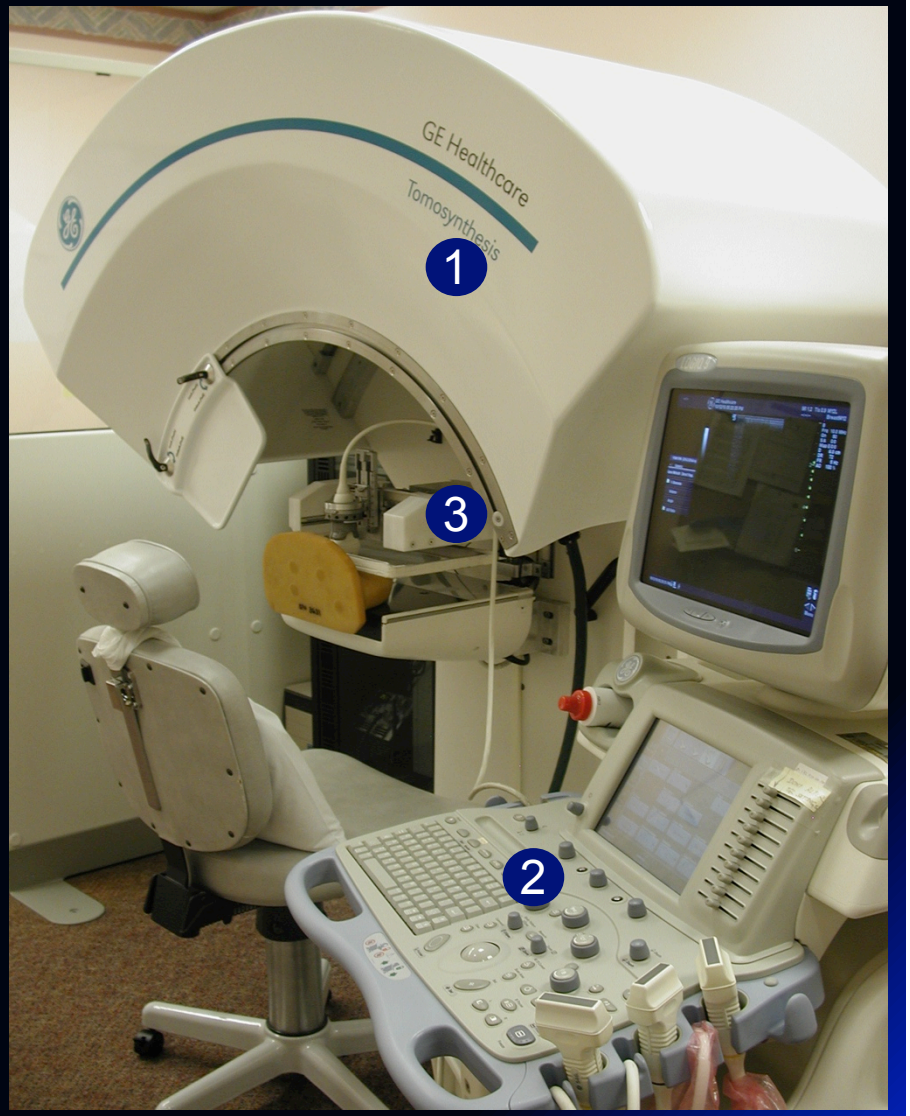

Multimodality breast imaging in same and different systems

Acquired scan

View from front-Elevational scan

Dual Sided MLO

Orthogonal Views

C-Scan MLO

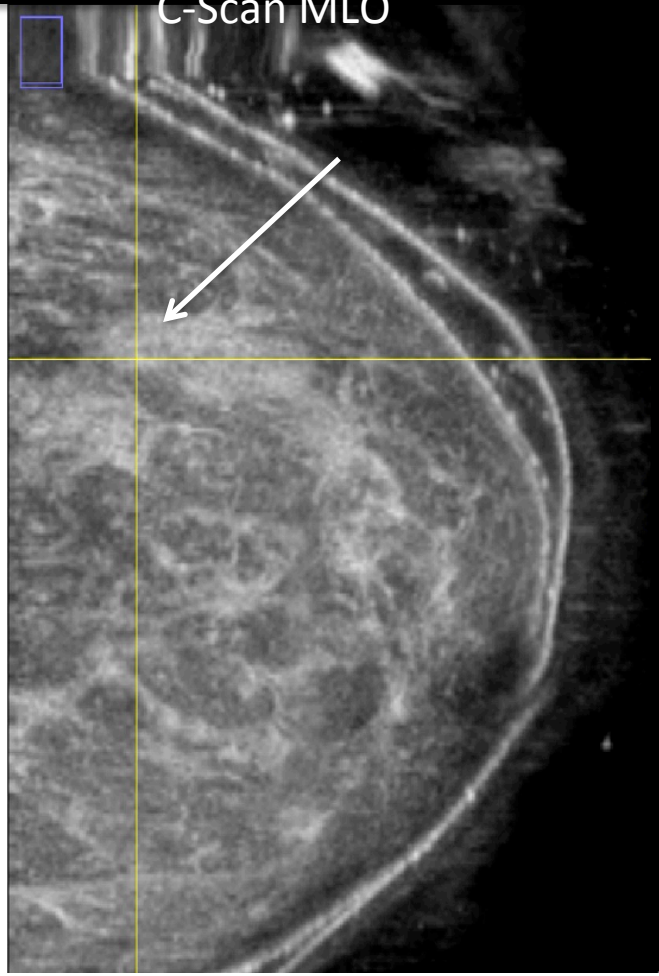

DBT density
Looks like glandular tissue on US in this case

- Acoustic coupling in the mammographic geometry - nearly solved
- Good 3D, aligned with DBT, within ~1 cm.
- Alignment is better when combined with the DBT system, facilitating mutually synergistic reconstructions.

DBT and Single and Dual Sided Breast Images with 38 mm wide transducer

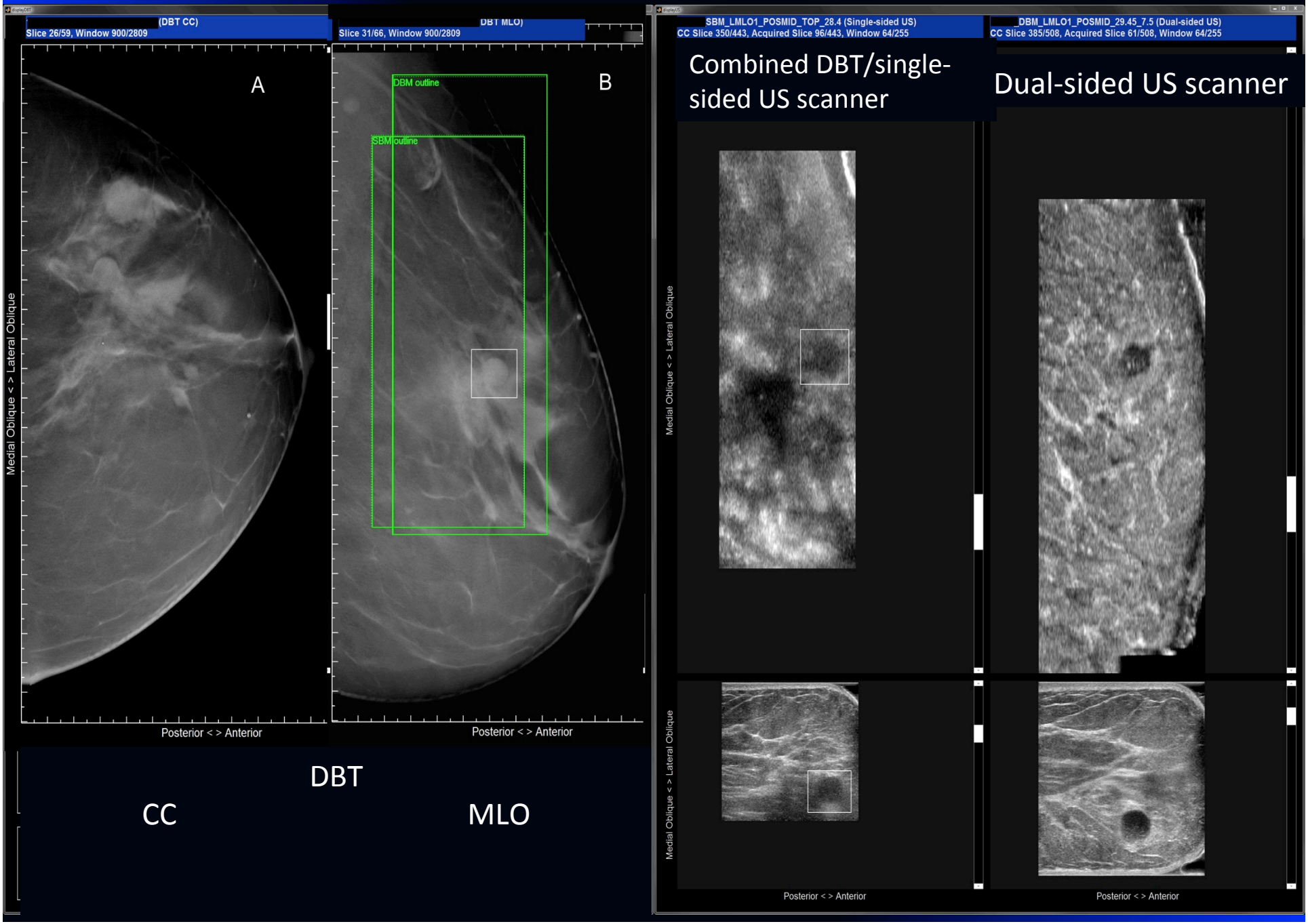

Contrast to noise increased 67% in dual sided images
7 cyst cases

Single sided Dualsided

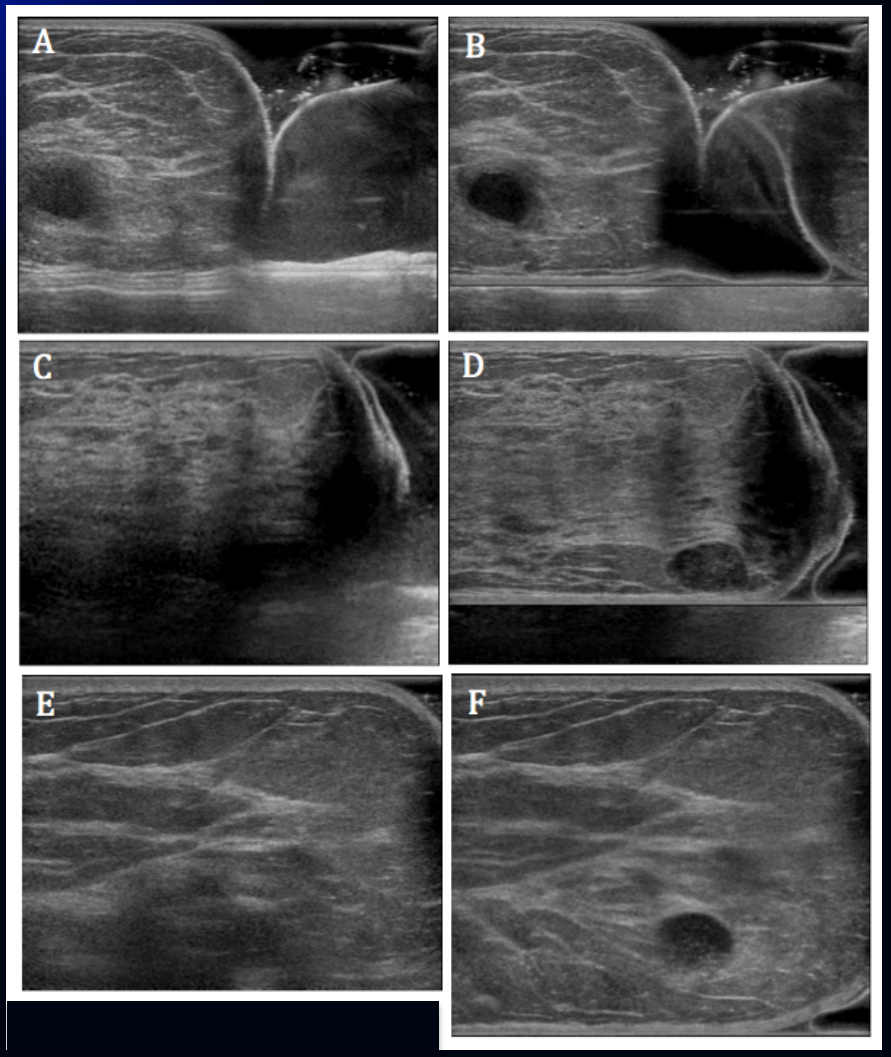

Case 1

Case 2

Case 3

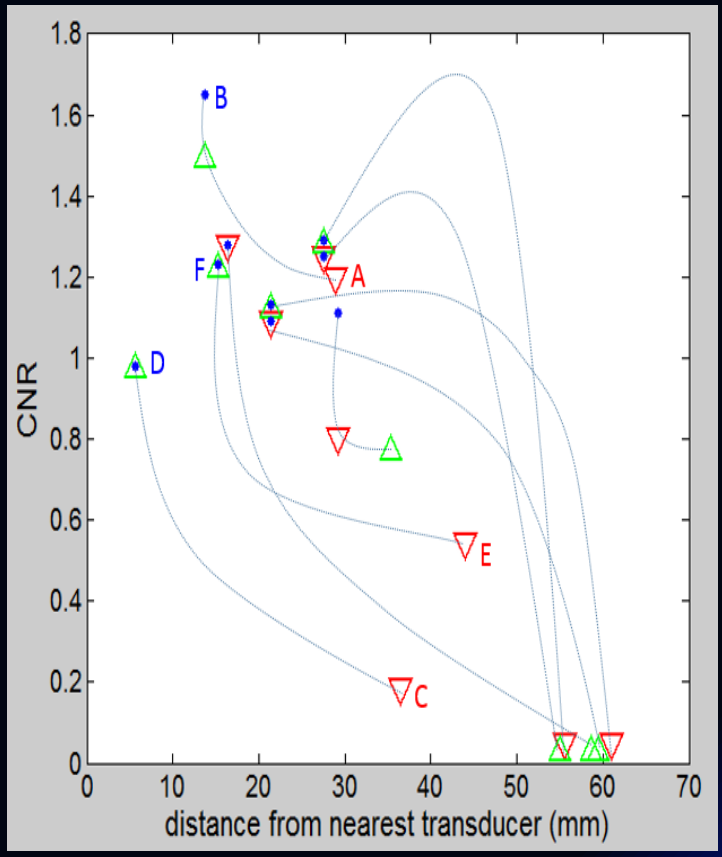

single sided TOP image (red downwards-pointing triangle), the single sided BOT image (green upwards-pointing triangle), and the dual sided TOPBOT image (blue dot)

Eric Larson, et al.

Fractional coverage of the breast

59% for imaging from the top or bottom only

89% for both)

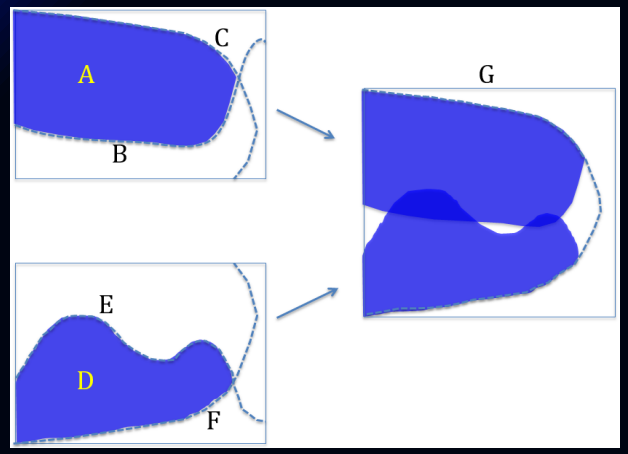

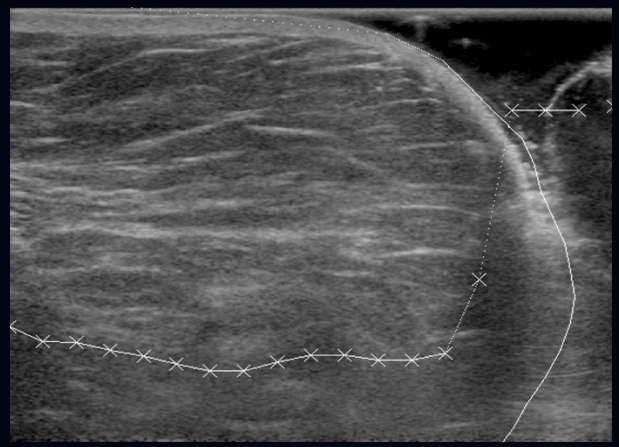

Fraction Covered (25 image sets)	Mean (%)	σ (%)
TOP	59.1	14.5
BOT	58.6	18.3
TOPBOT	89.1	12.2
Inter-reader Difference (25 image sets)	Mean (%)	σ (%)
TOP	-0.9	16.5
BOT	-4.8	18.9
TOPBOT	2.5	7.9
Intra-reader Difference (4 image sets)	Mean (%)	σ (%)
TOP	-2.5	6.4
BOT	-2.7	7.8
TOPBOT	0.6	0.8

Lobular CA In Situ

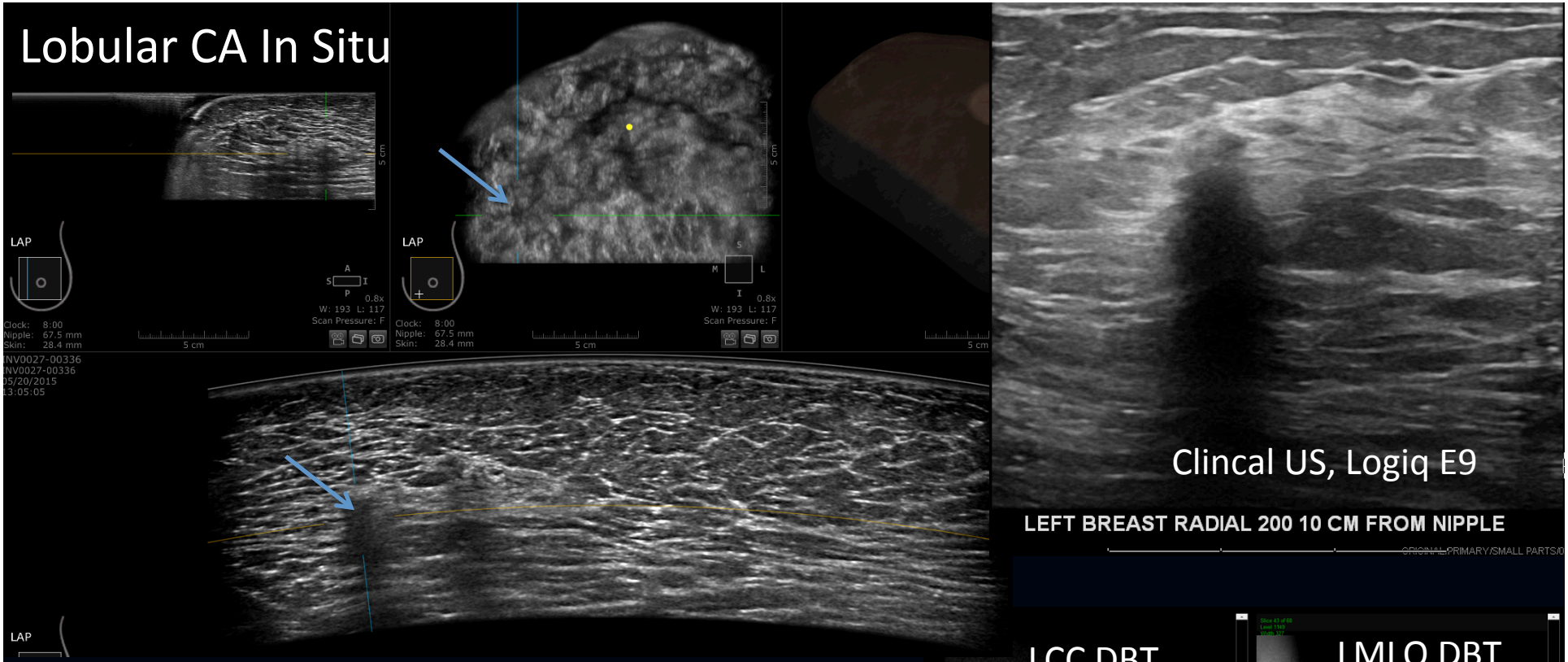

Long Array Fusion System

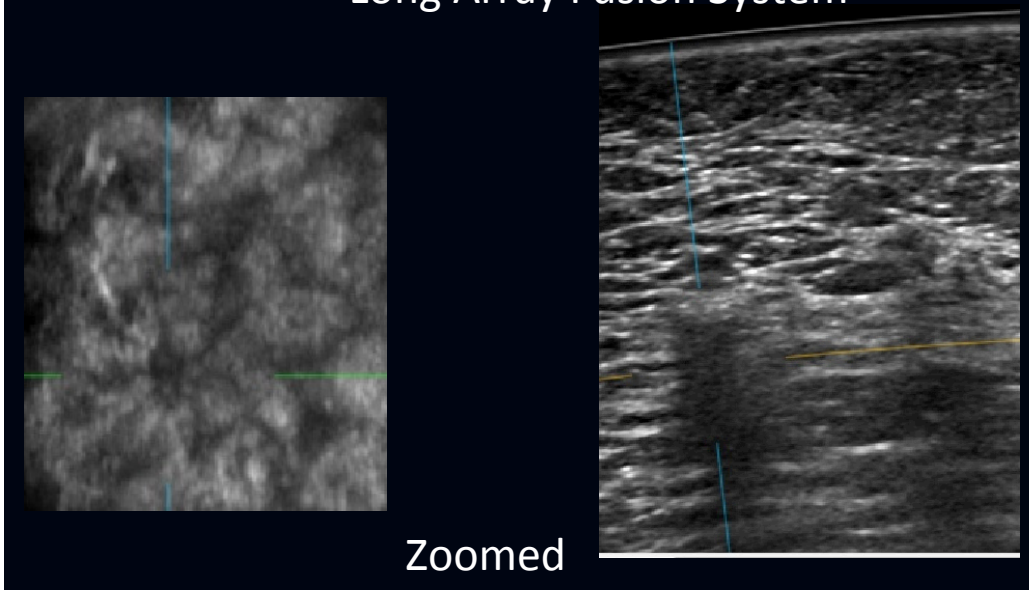

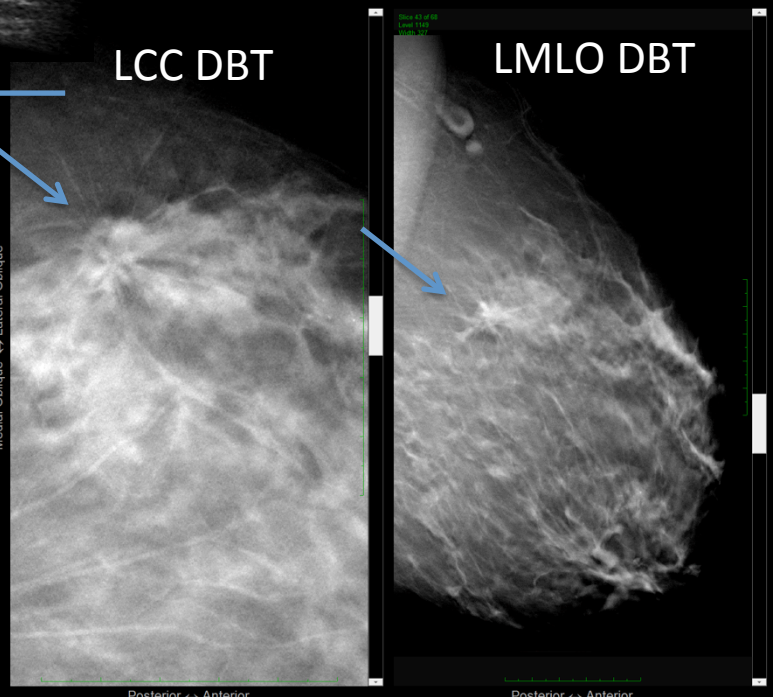

Sclerosing Fibroadenoma

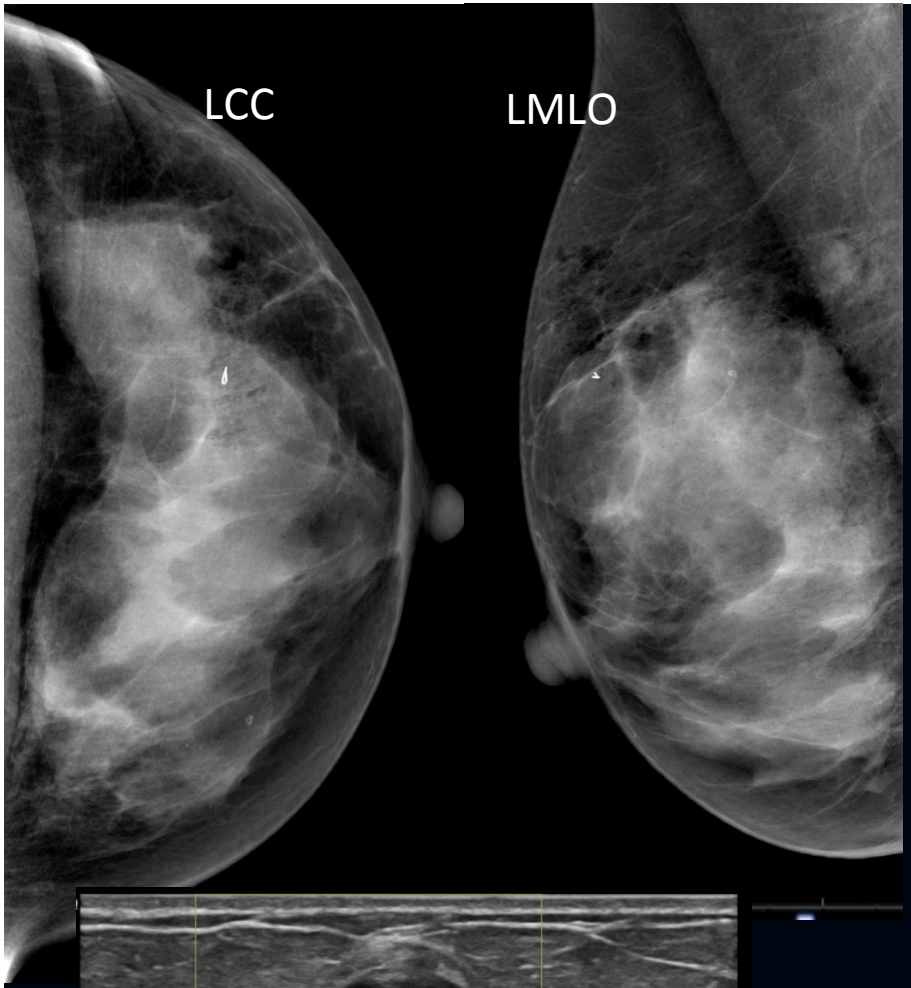

not visible on DBT, or mammo even with BX clips

Long Array Fusion System

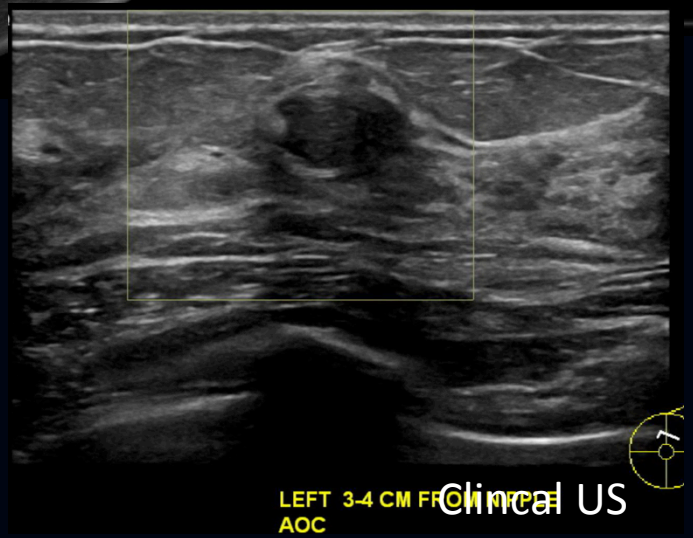

Clinical US

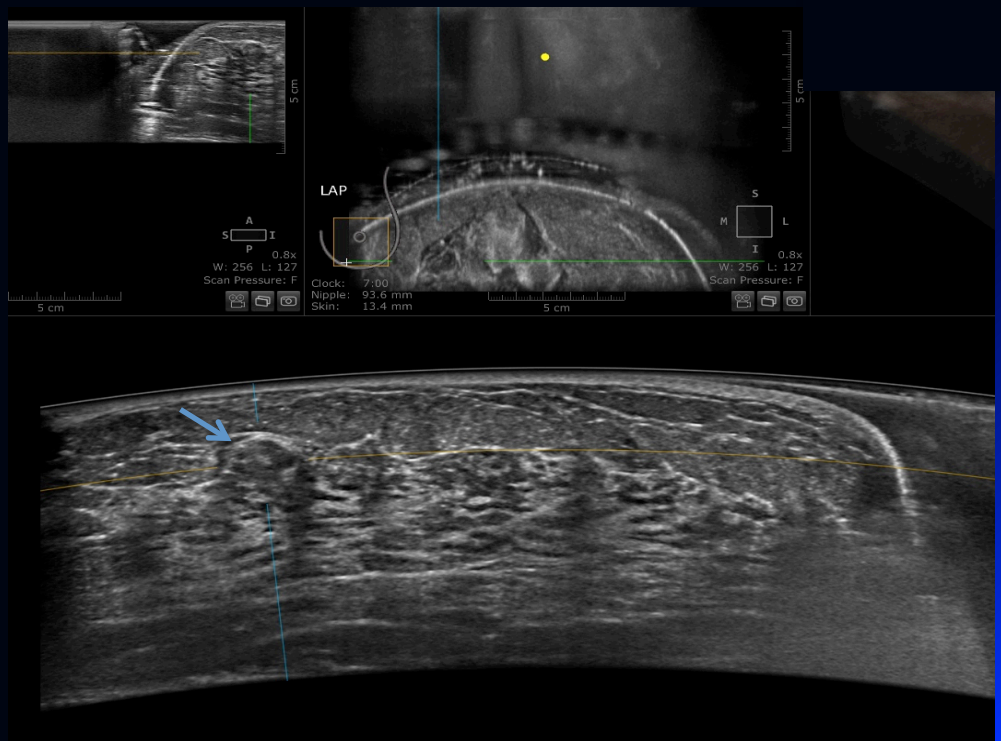

Existing Systems for SOS Imaging

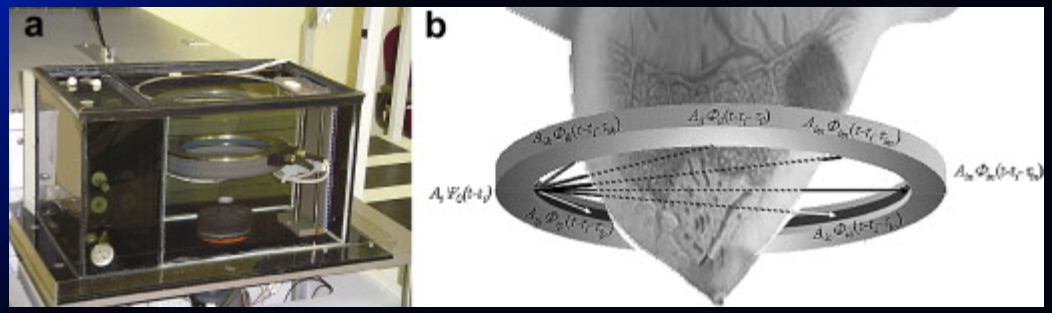

Delphinus

Techniscan

C. Li, N. Duric, P. Littrup, and L. Huang, "In vivo breast sound-speed imaging with ultrasound tomography." *Ultrasound in Medicine & Biology*, vol. 35, no. 10, pp. 1615-1628, Oct. 2009.

M. P. André, C. H. Barker, N. Sekhon, J. Wiskin, D. Borup, and K. Callahan, "Pre-Clinical experience with Full-Wave Inverse-Scattering for breast imaging acoustical imaging," ser. Acoustical Imaging, I. Akiyama, Ed. Dordrecht: Springer Netherlands, 2009, vol. 29, ch. 10, pp. 73-80.

Background

- Malignant lesions typically have an elevated sound speed and attenuation in comparison to breast fat tissue.

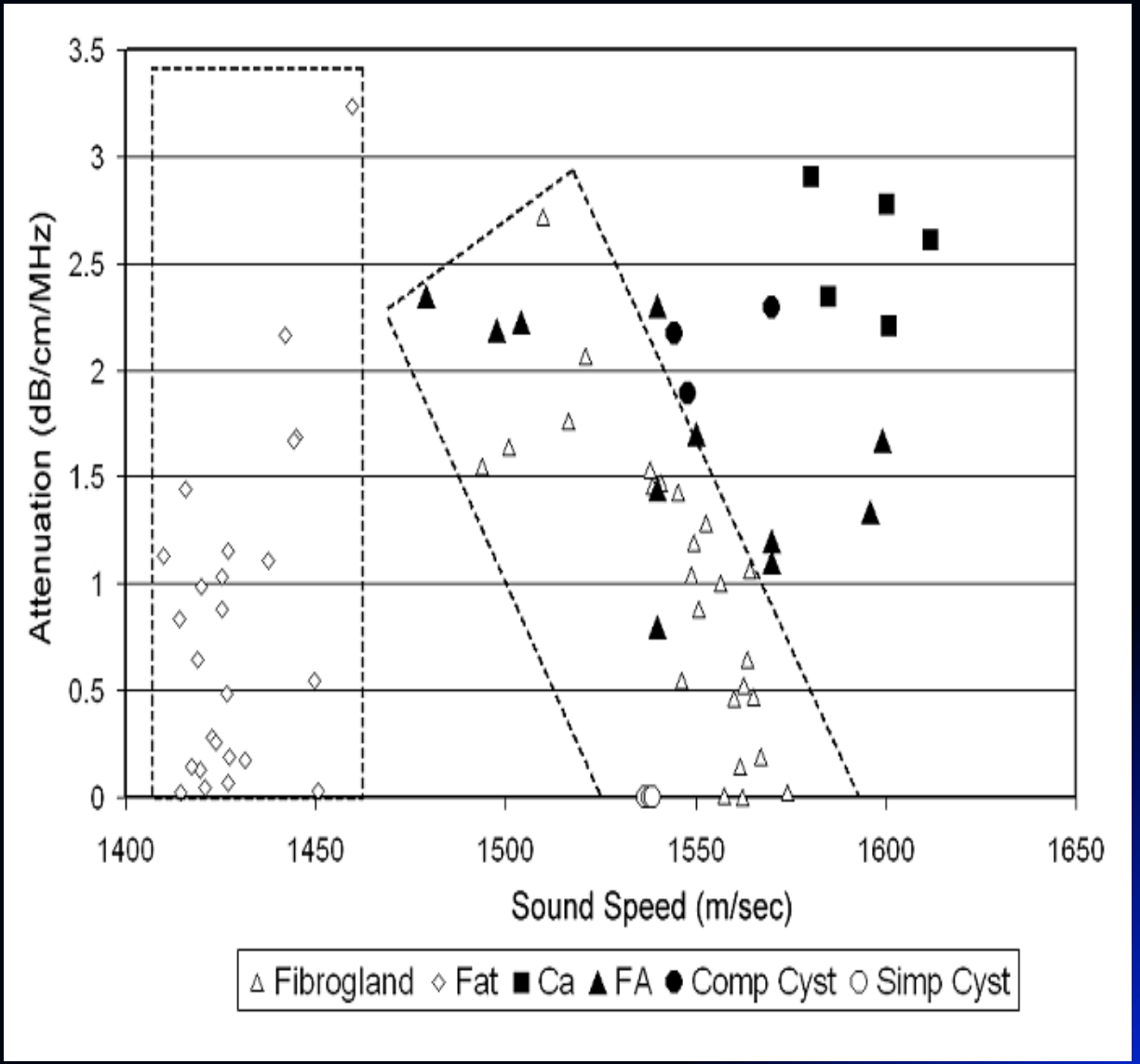

M. P. André, C. H. Barker, N. Sekhon, J. Wiskin, D. Borup, and K. Callahan, "Pre-Clinical experience with Full-Wave Inverse-Scattering for breast imaging acoustical imaging," ser. Acoustical Imaging, I. Akiyama, Ed. Dordrecht: Springer Netherlands, 2009, vol. 29, ch. 10, pp. 73-80.

The Dual Sided System, BLUCI

- Breast Light and Ultrasound Combined Imaging (BLUCI) employs opposed arrays operating in the compressed breast geometry
- Can do transmission tomography and PAT
- Co-registered to two-sided B-mode ultrasound
- Ready for coregistration to:
  - mammography
  - X-ray tomosynthesis
  - photoacoustics

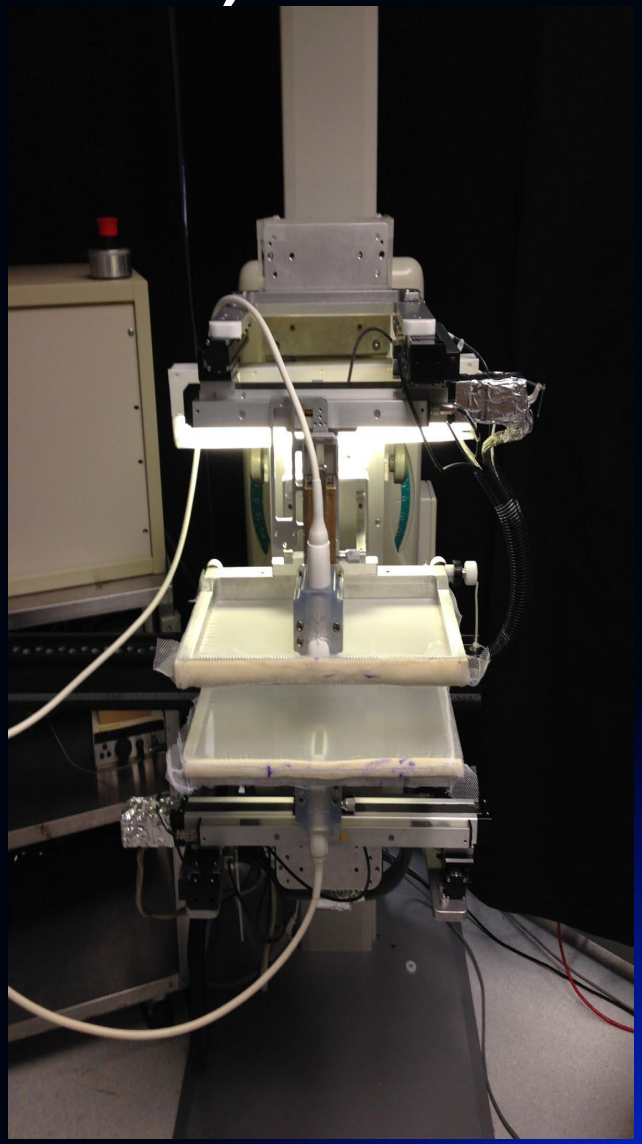

Sound Speed Image Reconstruction Algorithm for Ultrasound Limited Angle Tomography For Mammographic Geometry

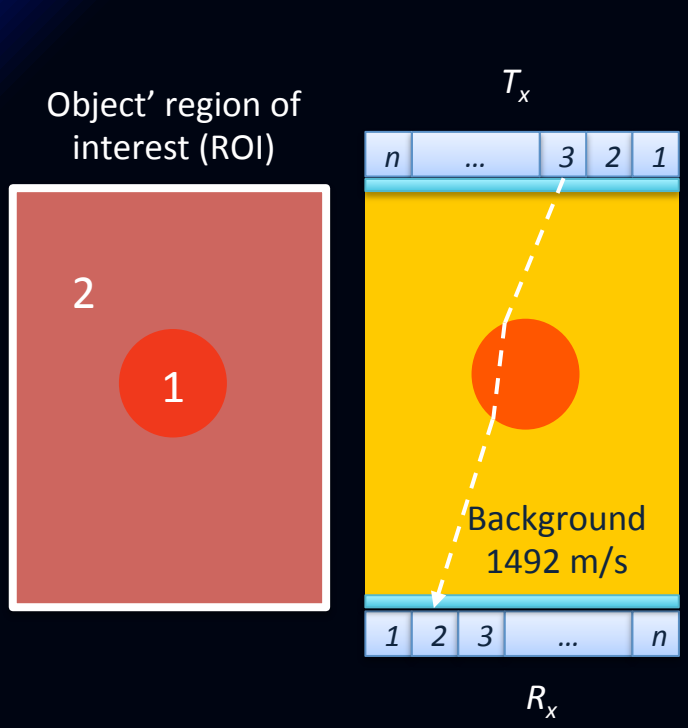

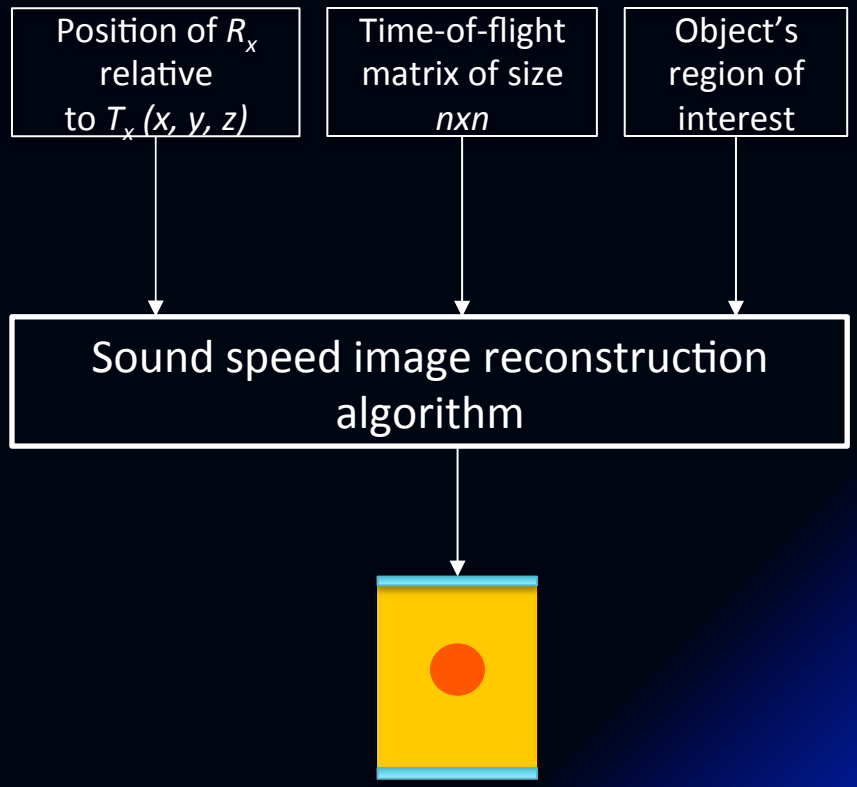

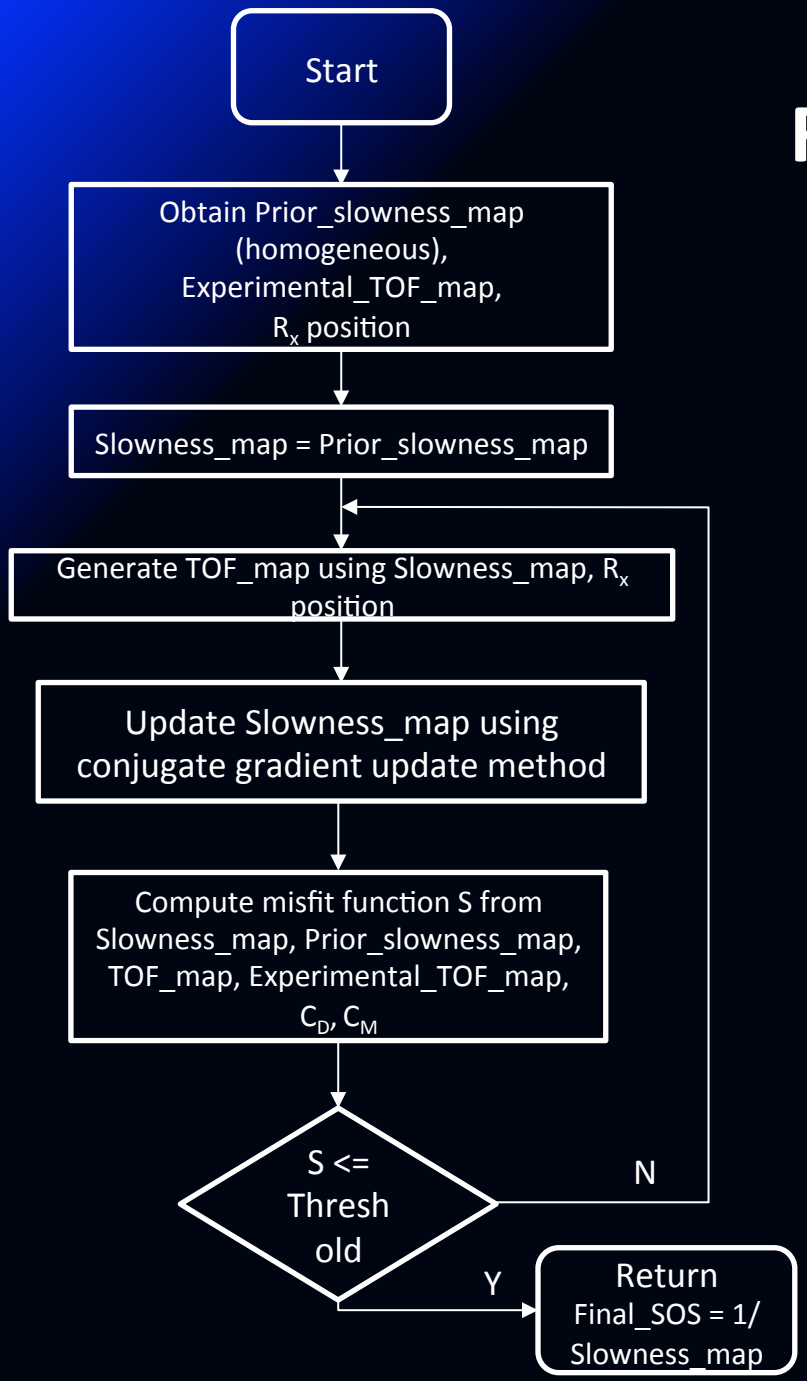

Ray Tracing Reconstruction

- Given:
  - Time-of-flight of all pairs of transmit and receive elements
  - Receive transducer' position
- Calculate
  - The slowness map

C_D: Data covariance matrix

TOF_map

Prior_slowness_map

$$= (g(m) - d_{obs})^T C_D^{-1} (g(m) - d_{obs}) + (m - m_{prior})^T C_M^{-1} (m - m_{prior})$$

Experimental_TOF_ map

Slowness_map

C_M: Model covariance matrix (ROI_map)

EXPERIMENT

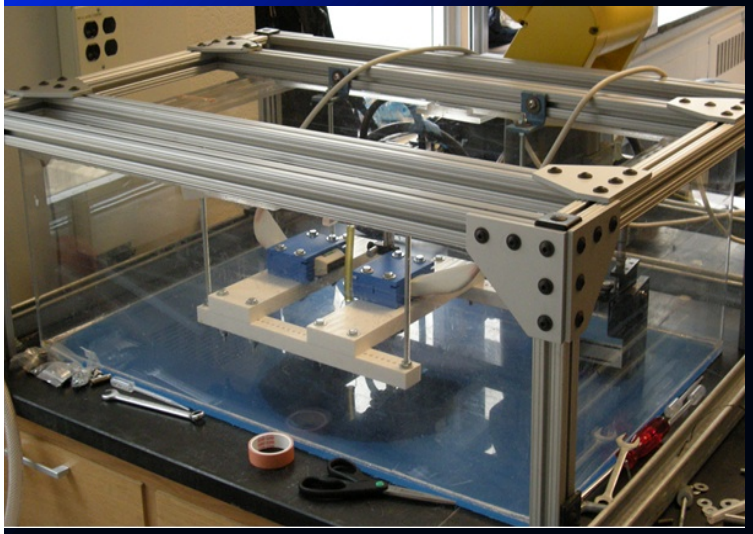

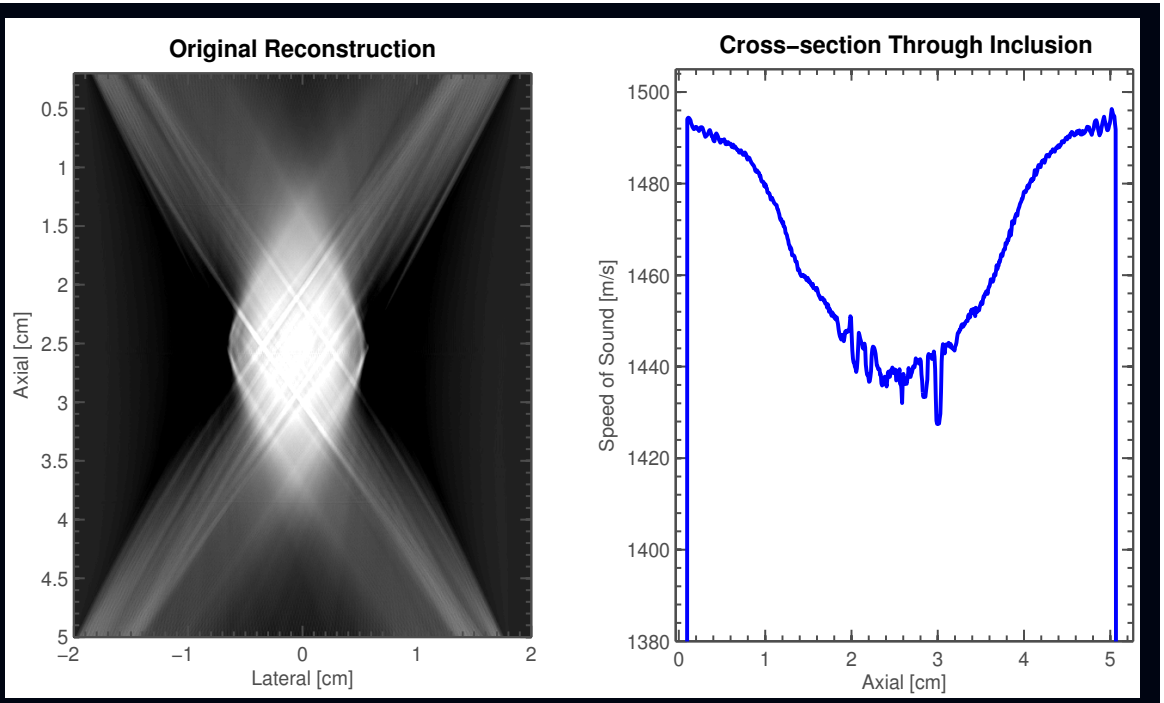

Precise forward model necessary for convergence

- Adequately fine grid spacing
- Knowledge of transducer locations
- Incorporate lens information in the forward model

A priori information from pulse echo

- Can make limited angle SOS quantitative

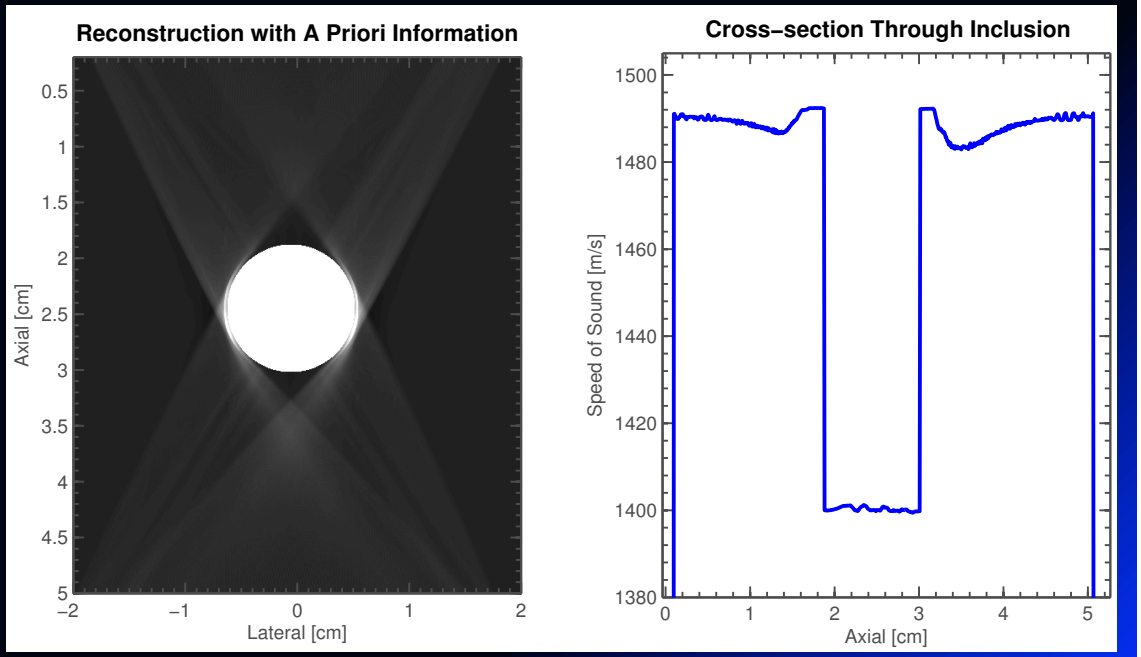

- Madsinh phantom

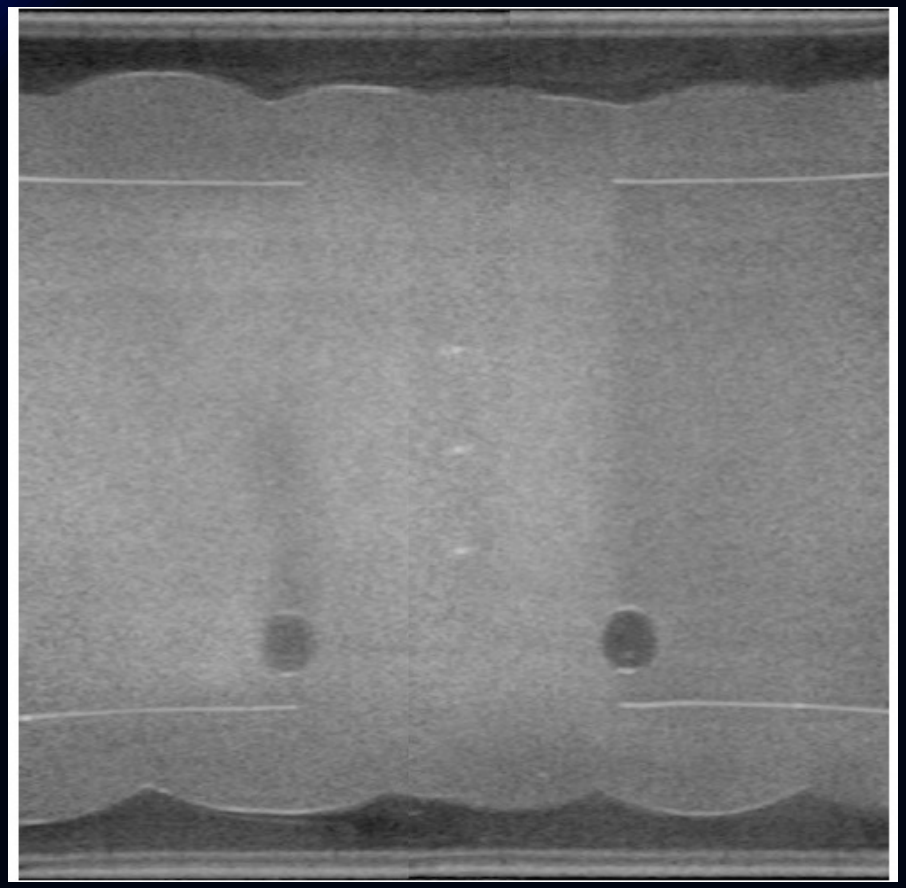

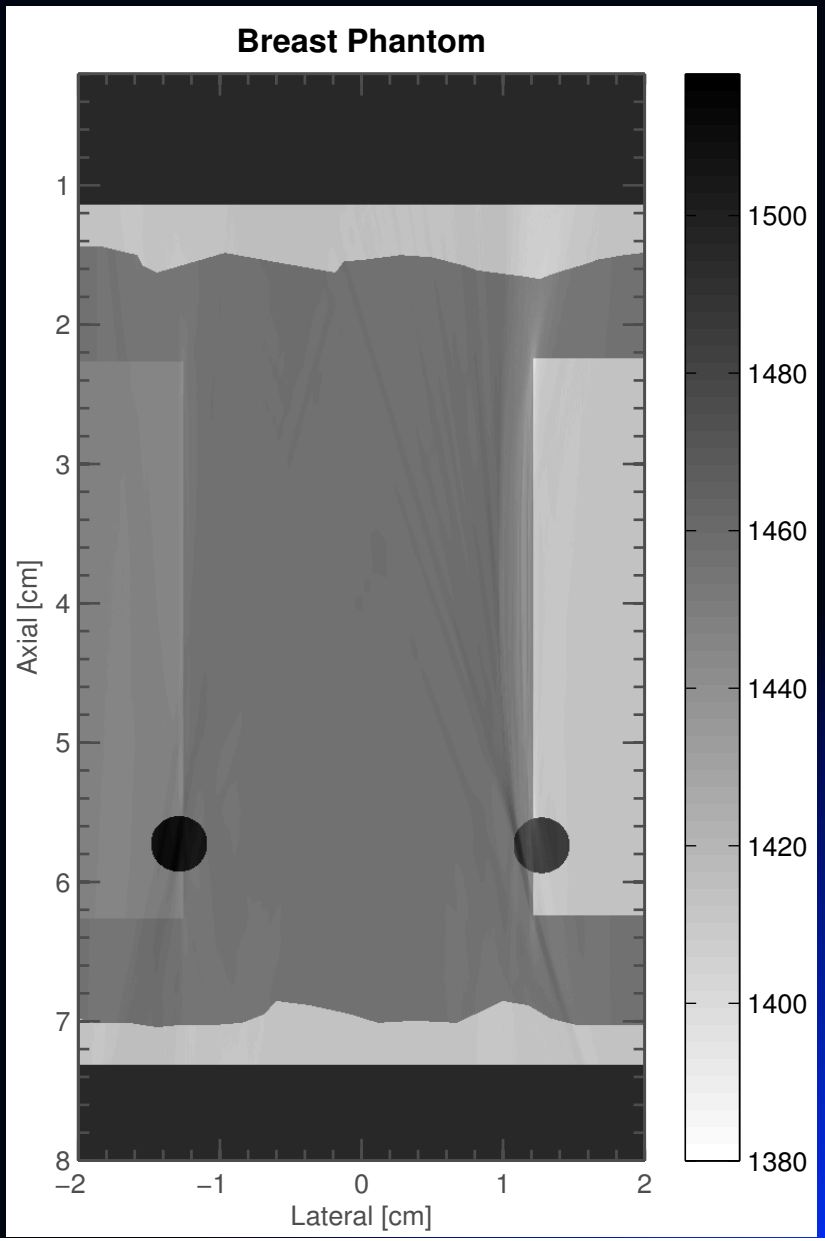

Limited angle attenuation images, with L4-7 transducer, of an attenuating, 12 mm dia., cylinder in water using a weighted least squares model with a priori information

Uncorrected

Hooi FM, "Optimized beamforming and limited angle tomography of the compressed breast," dissertation, Univ. of Michigan, 2012, Ann Arbor, pp. 114, MYNCBI 99826424.

Corrected

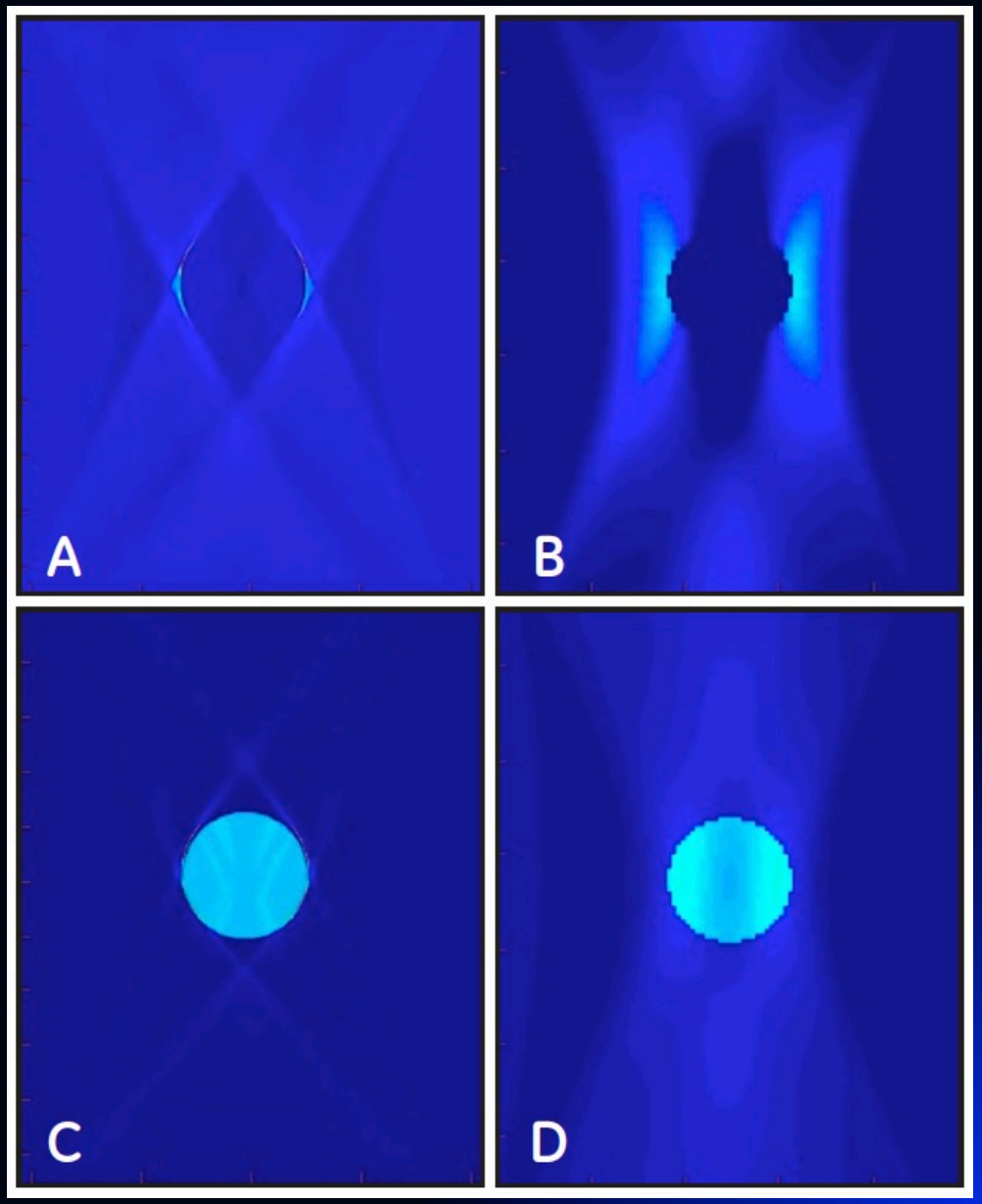

Segmentation in Real Breasts

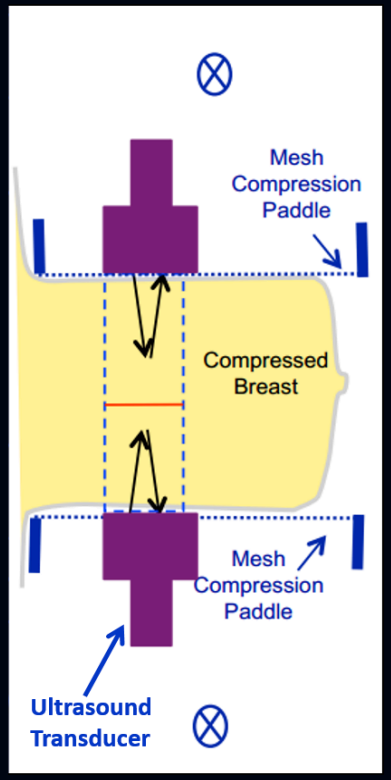

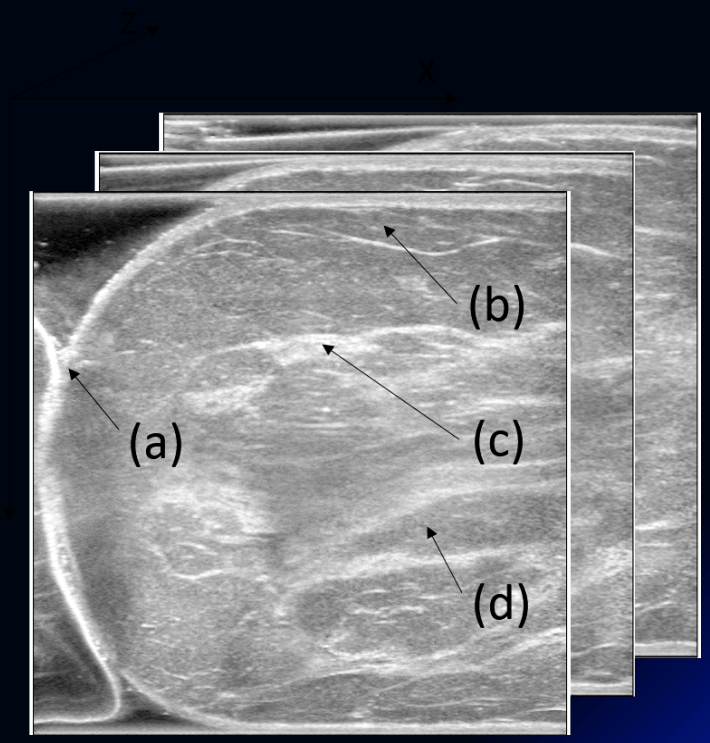

acquired view of the data with the coordinate system. (a) Skin, (b) subcutaneous fat, (c) glandular tissue and (d) fat.

segmentation approach

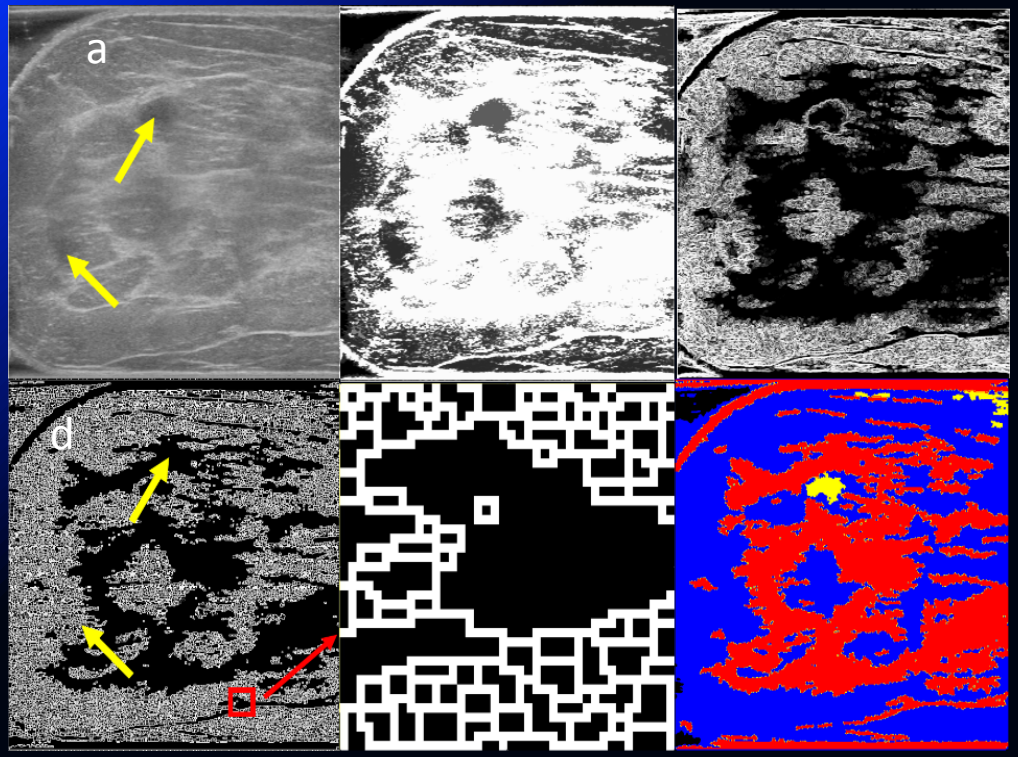

(1) morphological processing, to eliminate the speckle noise
(2) edge information extraction;
(3) watershed segmentation;
(4) region classification

Region classification based on features of mean intensity histogram

(b) Opening-by-reconstruction and closing-by-reconstruction in 3D space
(c) Application of 3D sobel operator
(d) Watershed boundaries in image space
(e) Detail of d
(e) Tissue-specific region classification

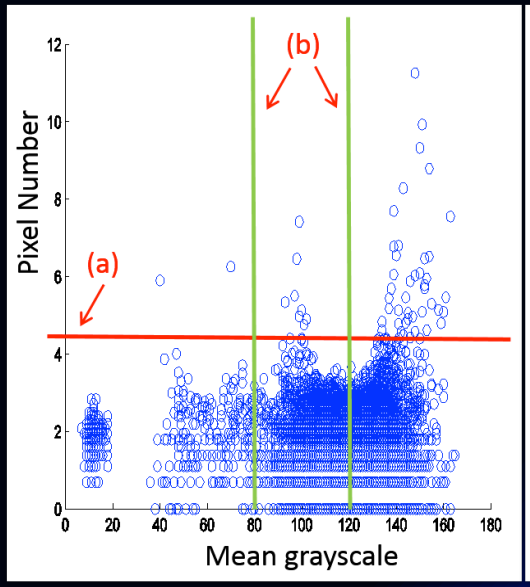

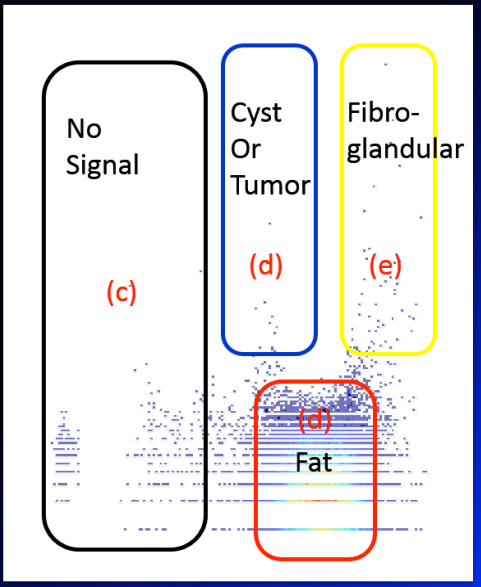

Manually supervised and corrected and automated segmentations of fibroglandular tissues

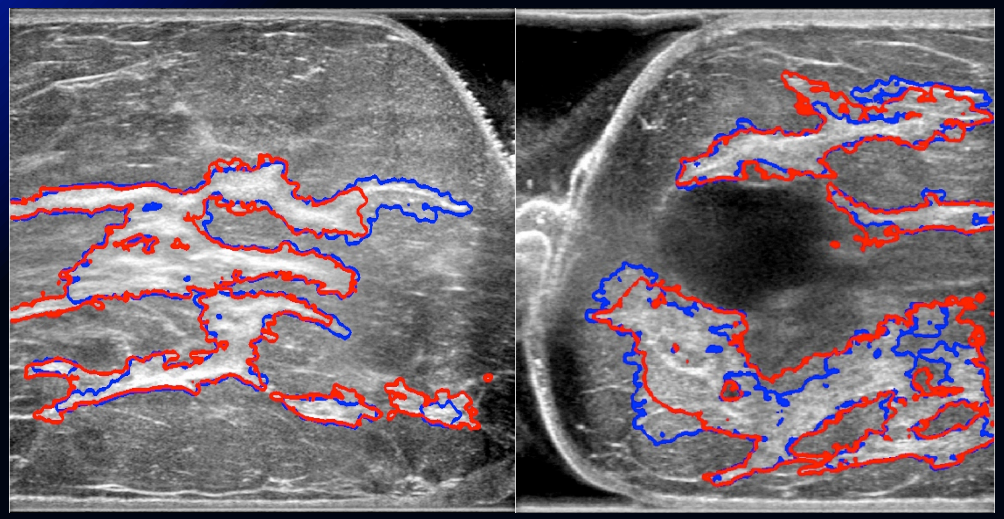

Automated segmentation agreed with BIRADS classification by radiologist in 86% of 21 cases.

Manually supervised and corrected classification on 8 cases showed good Pixel by pixel agreement.

Table 1. Quantitative comparison of manual segmentation and automated segmentation

Test image	1	2	3	4	5	6	7	8	Average
SE(%)	6.32	10.15	9.98	8.01	7.64	8.57	5.14	9.33	8.14
TC(%)	79.68	70.28	71.44	71.95	76.28	71.63	80.55	70.28	74.54

SE -- misclassified pixels as % of all breast pixels
TC – Intersection of sets of manual and automated segmented pixels/ union of those sets

Peng Gu, Won-Mean Lee, Marilyn A. Roubidoux, Jie Yuan, Paul L. Carson

Limited Angle Ultrasound Tomography

- Less than perfectly rigid scanning system
- Application: combination with X-ray

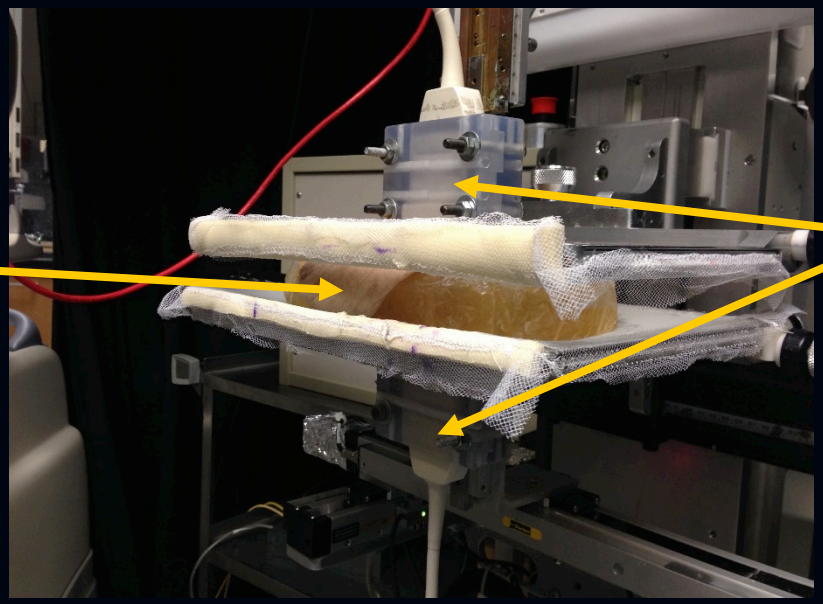

Jintamethasawat, Kripfgans, *et al.*

- Errors from *a priori*: **segmentation misalignments**
- Errors from poor system calibration*:* **transducer misalignments**
- If cannot eliminate errors, how much error the imaging system can tolerate?

Limitations

- Breast specimen reconstruction example

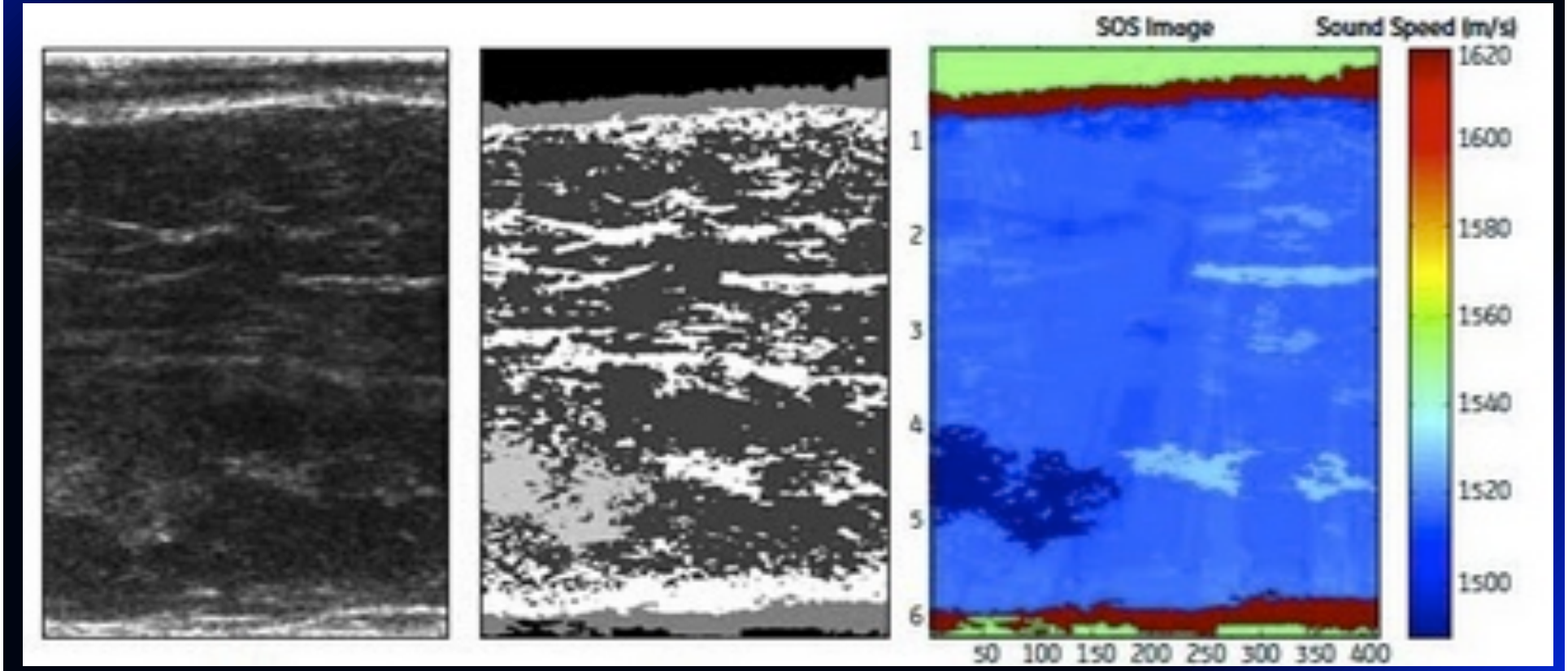

Conclusions

- Estimated maximum misplacement allowed in each imaging scenario (9 mm object diameter)

Misplacement type/ Imaging scenario	20 m/s Fat-water discrimination	5 m/s Fine discrimination	0.5ºC Hyperthermia monitoring
Segmentation size	6 mm	1 mm	0.2 mm
Segmentation location in lateral direction	> 5 mm, < -5 mm	2 mm	0.4 mm
Segmentation location in axial direction	> 5 mm, < -5 mm	5 mm	1 mm
Transducer translational misplacement in axial direction	0.2 mm	35 µm	7 µm
Transducer translational misplacement in lateral direction	4 mm	1 mm	0.2 mm
Rotational misalignment about elevational axis	> 10 deg, < -10 deg	2 deg	0.4 deg
Transducer translational misplacement in elevational direction	5 mm	2 mm	0.4 mm
Rotational misalignment about axial axis	> 10 deg, < -10 deg	> 10 deg, < -10 deg	> 10 deg, < -10 deg

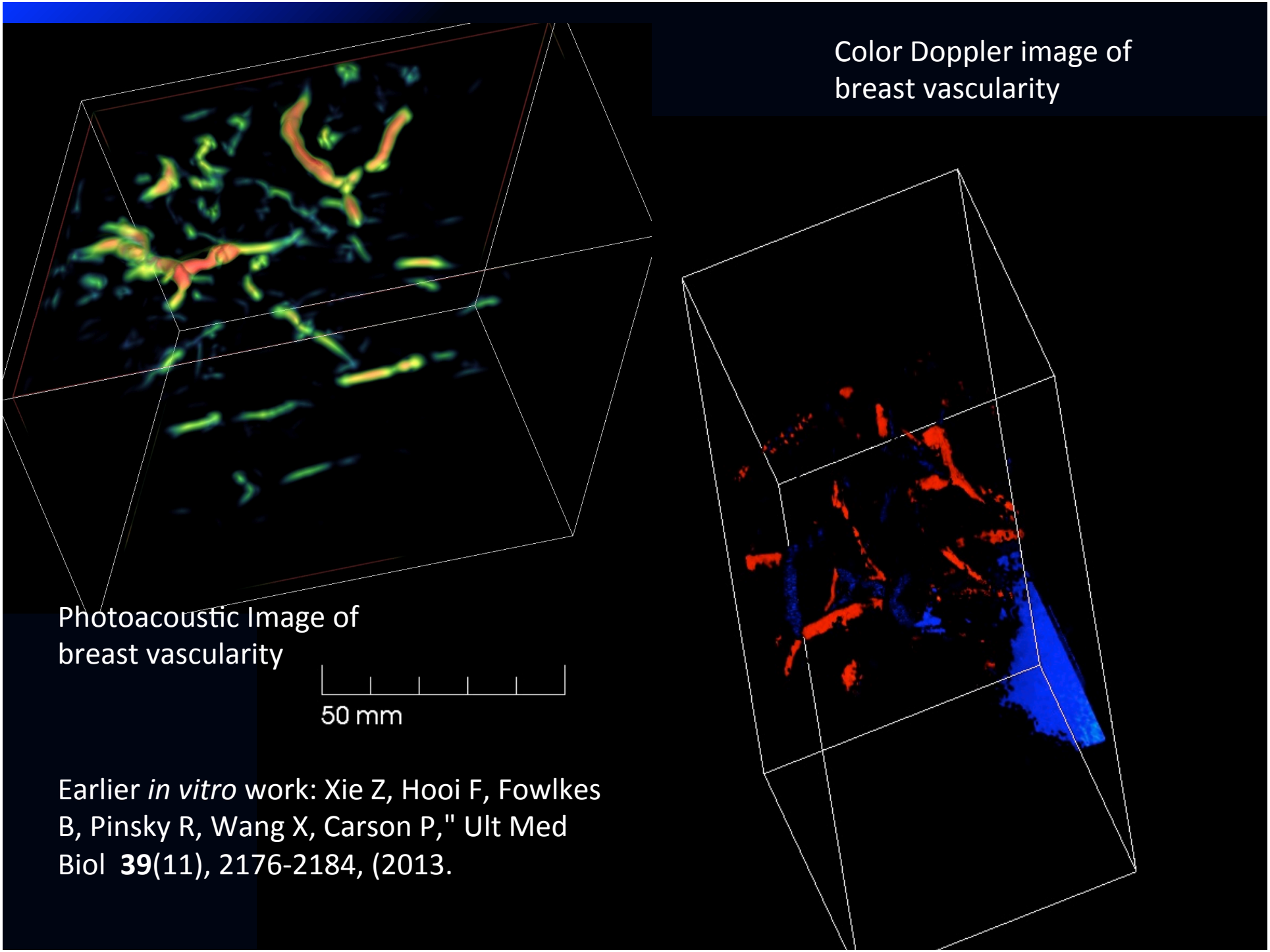

Earlier *in vitro* work: Xie Z, Hooi F, Fowlkes B, Pinsky R, Wang X, Carson P," Ult Med Biol **39**(11), 2176-2184, (2013.

Acknowledgements

This work was supported in part by:

- NIH BRP 1 R01 CA115267, NIH BRP 2 R01 CA91713, and NSF CBET 0756338.

Many more deserve acknowledgement, including:

Sushma Alvar

Sacha Verweij

Mark Haynes

Kai Thomenius

Cynthia Davis

Larry Mo

et al.